Sensitivity of the Modeled North American Monsoon Regional Climate to Convective Parameterization

DAVID J. GOCHIS

Department of Hydrology and Water Resources, The University of Arizona, Tucson, Arizona

W. JAMES SHUTTLEWORTH

Department of Hydrology and Water Resources and Department of Atmospheric Sciences, The University of Arizona, Tucson, Arizona

ZONG-LIANG YANG

Department of Hydrology and Water Resources, The University of Arizona, Tucson, Arizona

ABSTRACT

This paper documents the sensitivity of the modeled evolution of the North American monsoon system (NAMS) to convective parameterization in terms of thermodynamic and circulation characteristics, stability profiles, and precipitation. The convective parameterization schemes (CPSs) of Betts–Miller–Janjic, Kain–Fritsch, and Grell were tested using version 3.4 of the PSU–NCAR fifth-generation Mesoscale Model (MM5) running in a pseudoclimate mode. Model results for the initial phase of the 1999 NAM are compared with surface climate station observations and seven radiosonde sites in Mexico and the southwestern United States. The results show substantial differences in modeled precipitation, surface climate, and atmospheric stability occuring between the different model simulations, which are attributable to the representation of convection in the model. Moreover, large intersimulation differences in the low-level circulation fields are found. While none of the CPSs tested gave perfect simulation of observations everywhere in the model domain, the Kain–Fritsch scheme generally gave significantly superior estimates of surface and upper air verification error statistics.

1. Introduction

The application of regional climate models (RCMs) has increased dramatically since their inception (Dickinson et al. 1989; Giorgi 1990; Giorgi and Mearns 1999), as have studies conducted to assess the sensitivity of modeled regional climate to changes in surface forcing (e.g., Small 2001; Giorgi and Marinucci 1996; Giorgi and Shields 1999; Copeland et al. 1996) and model physics (e.g., Wang and Seaman 1997; Giorgi and Marinucci 1996). Sensitivity to physical parameterization, parameter values, grid and domain size (Seth and Giorgi 1998), and boundary forcing greatly complicates the implementation of regional climate models. Model verification is therefore essential, but may well be complicated by differences between the grid used in the RCM and that of the analyzed fields of observational data used for verification, and by the fact that reanalyzed datasets may contain similar physical parameterizations (and biases) as the model being evaluated. Conversely, reanalyzed datasets may contain disparaging biases associated with totally different physical parameterizations.

The adequate representation of convective processes is particularly important in RCMs, but there is no universally accepted framework for representing convection in numerical simulation models operating with grid scales that prohibit fully explicit representation. In fact, the representation of convection is strongly scale dependent (Molinari and Dudek 1992), and several different convective parameterization schemes (CPSs) have been developed that implicitly account for the associated subgrid exchanges of mass, heat, and moisture. The differences in these formulations have a pronounced influence on numerical modeling results (e.g., Wang and Seaman 1997; Giorgi and Shields 1999; Zhang and McFarlane 1995; Giorgi and Marinucci 1996) and vary with the convective environment being simulated. To date, there has been no comprehensive assessment of CPS performance in simulating deep convection over the southwest United States and Mexico.

The Pennsylvania State University–National Center for Atmospheric Research (PSU–NCAR) fifth-genera-

Corresponding author address: David Gochis, Department of Hydrology and Water Resources, The University of Arizona, Harshbarger Building 11, Tucson, AZ 85721.
E-mail: gochis@hwr.arizona.edu

tion Mesoscale Model (MM5) (and similar modeling systems) is being increasingly recognized as critical in operational hydrometeorological prediction systems. However, there have been no definitive publications offering guidance on the relative performance of CPSs in MM5 over the North American monsoon (NAM) region, although a preliminary study by Gochis et al. (2000) suggested that substantial differences were likely [for a thorough description of the NAM, see Douglas et al. (1993), Adams and Comrie (1997), or Higgins et al. (1997)]. Basic convective research (e.g., Kain and Fritsch 1990) indicates that differing representations of subgrid convection yields not only different amounts of precipitation but also differing degrees of atmospheric heating due to parameterized latent heat exchanges. With regard to the NAM system (NAMS), Barlow et al. (1998) concluded that residually derived, mid- and upper-tropospheric diabatic heating attributed to convection plays a significant role in developing the NAM circulation. Thus, the primary goal of this study was to provide quantitative assessment of three CPSs available in the MM5 model (Grell et al. 1994) and to document through verification and sensitivity analyses the relative performance of these CPSs when simulating the NAMS. In this paper, we refine the previous study by Gochis et al. (2000) by (a) extending the internal nested domain used in MM5 to approximately 120°W; (b) allowing sea surface temperature to vary, these being updated every 6 h along with the lateral boundary conditions; and (c) including a third convective parameterization, the Betts–Miller–Janic scheme, in the comparison along with the Kain–Fritsch and Grell schemes.

Section 2 briefly describes the model configuration and simulation and verification procedures (the appendix provides a brief description of each of the three CPSs). The results are presented in section 3 and discussed in section 4. Section 5 gives concluding comments.

2. Model and analysis methods

a. The MM5 model

The PSU–NCAR MM5 version 3.4 (Grell et al. 1994) consists of a nonhydrostatic dynamic core and a suite of optional physical parameterizations integrated on a terrain-following, sigma, vertical coordinate system. A two-way interacting nested configuration (90 and 30 km) was used in this study, with the coarse domain covering approximately 10°–45°N and 125°–85°W and the fine domain covering most of Mexico and the southwestern United States (see Fig. 1). The model was integrated continuously from 0000 UTC 16 May through 0000 UTC 2 August 1999, while the lateral boundary forcing for the coarse domain was one-way and was provided by the National Centers for Environmental Prediction (NCEP)–NCAR reanalysis dataset (Kalnay et al. 1996). Model sea surface temperatures (SSTs) tak-

en from the weekly dataset of Reynolds and Smith (1994) were linearly interpolated to 6-hourly values and used as lower boundary conditions. The model output was saved every 3 h for analysis. Because only the results for the month of July were compared, the spinup period for the simulations is on the order of 6 weeks. As suggested by Giorgi and Mearns (1999), this should be more than adequate for thorough propagation of lateral boundary conditions, but may not be adequate for a full spinup of certain land surface conditions such as soil moisture, hence our use of the phrase "pseudoregional climate simulations" to describe our modus operandi. Other significant model options used in this study are listed in Table 1.

The three different CPSs selected for study in this sensitivity experiment were the schemes of Betts–Miller (Betts 1986; Betts and Miller 1986) as implemented by Janjic (1994), hereafter referred to as BMJ, of Grell (Grell 1993; Grell et al. 1994), hereafter referred to as GR, and of Kain–Fritsch (Kain and Fritsch 1990), hereafter referred to as KF. These schemes vary in their representation of physical processes (see the appendix), ranging from the relatively simple profile adjustment scheme of BMJ to the entraining–detraining mass flux scheme of KF. The schemes also vary in their formulation of convective initiation ("trigger function") as well as their criteria for convective termination ("relaxation"). All of the CPSs have been implemented and tested in the MM5 modeling framework and have shown success in simulating convection at the 20–40-km grid resolution (Giorgi and Shields 1999; Janjic 1994; Kain and Fritsch 1990) in climates such as the North American Great Plains. A brief description of each CPS is given in the appendix, but readers are referred to the articles given above for more thorough descriptions of the individual schemes.

Assumptions in the GR and KF formulations preclude their application at the coarse domain grid of 90 km. Consequently, the BMJ scheme, which does not possess the same scale-limiting assumptions as the GR and KF schemes, was always used for the intermediate 90-km grid. Thus, the only difference between the simulations was that convective processes were represented by the BMJ, GR, and KF schemes within the internal 30-km domain. In each case, the default parameters for each CPS were used. As discussed later, this may impact the results of the sensitivity study. Although the model was integrated from mid-May through July, only the results for July are presented here because convective activity is much more prevalent throughout the NAM region in July than it is during June, and the intersimulation differences for June were not definitive.

b. Evaluation of upper-level climate

The differences in the monthly mean profiles of temperature, specific humidity, equivalent potential temperature, and wind at specified levels were calculated
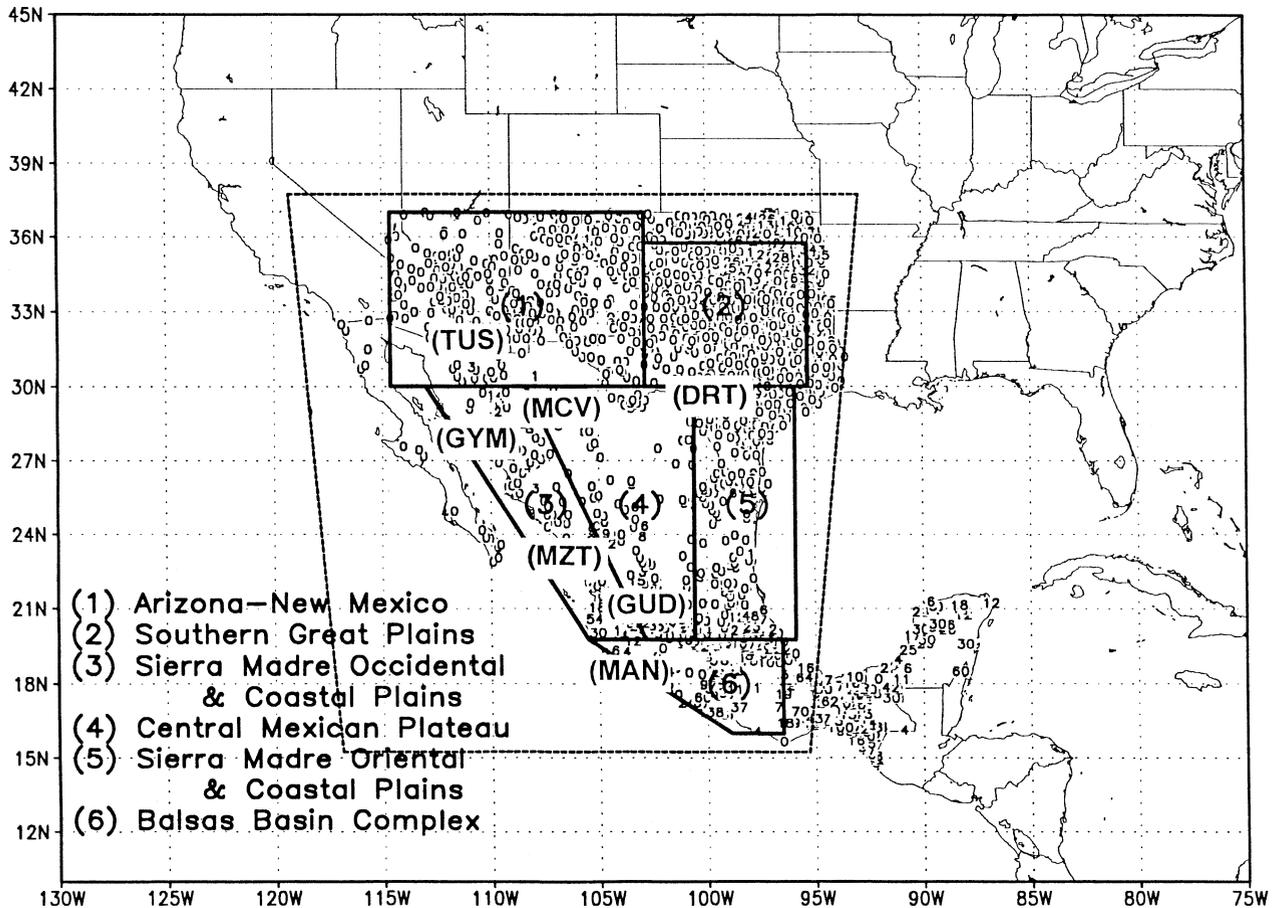
FIG. 1. Coarse (90 km, approximately map frame) and fine (30 km, dotted line) domains. Solid lines: physiographically similar areas used in the calculations of regional verification statistics. Small numbers indicate locations of daily precipitation gauges. Bold letters indicate radiosonde station locations.

between the model and five sounding observations in Mexico, specifically at Chihuahua (MCV), Guaymas (GYM), Mazatlan (MZT), Manzanillo (MAN), and Guadalajara (GUD), and at two sounding observations in the United States, specifically at Tucson, Arizona (TUS), and Del Rio, Texas (DRT). Observational soundings were obtained from the online archive maintained by the National Oceanic and Atmospheric Administration's (NOAA) Forecast Systems Laboratory. These observations undergo extensive gross error and hydrostatic consistency checks prior to being archived. No spatial averaging was performed on these upper air variables. Bias is expressed as the July mean model minus July mean observed soundings, the modeled values having been selected to correspond to the time of the sounding, that is, 1200 UTC for GYM, MAN, DRT, and TUS, and 0000 UTC for MCV and MZT. Although both 0000 and 1200 UTC observations were available for TUS and DRT, the 1200 UTC sounding was selected for use in the analysis because it is suspected to be less contaminated by afternoon convection. In addition to the station verification, spatial plots of pressure-integrated wind

TABLE 1. Model options used in the sensitivity experiments.

Physics option	Model setup
Explicit microphysics	Simple ice (Grell et al. 1994)
Land surface model	Oregon State University/Eta Model (Chen and Dudhia 1999)
PBL	Medium Range Forecast Model (Hong and Pan 1996)
Radiation	Cloud radiation scheme (Grell et al. 1994)
Cumulus (90-km domain)	Betts–Miller–Janjic (Janjic 1994)
(30-km domain)	Kain–Fritsch (Kain and Fritsch 1990)
	Grell (Grell et al. 1994)
	Betts–Miller–Janjic (Janjic 1994)

and divergence, column-integrated precipitable water, and monthly total precipitation were also constructed to aid discussion of the differences between the model simulations. (Note: detailed analyses of moisture transport features and hydrologic fluxes are the subject of a forthcoming paper.)

c. Evaluation of surface climate

The model-calculated, near-surface, daily average air temperature, T_{av}, and dewpoint temperatures, T_d, at 2 m above ground level were compared to surface station observations obtained from the National Climate Data Center's (NCDC) Global Surface Summary of the Day historical archive. These data are quality controlled by the United States Air Force through a variety of automated routines. No correction was made for the differences between grid and station elevation, which may introduce systematic bias into the error estimates, as discussed in section 3. However, we believe this does not change our overall conclusions on the relative merits of the schemes considered in this study. Paired samples of modeled and observed air and dewpoint temperatures were constructed for each station location by spatially averaging all of the available station and gridpoint values within 1° radius of each station and the center of each corresponding model grid cell. Errors calculated as model values minus observed values for each station were then averaged for the entire month of July. Precipitation statistics were calculated in the same way, except that monthly total station rainfalls were used rather than daily values. The rainfall data were daily total rainfall observations from Mexico and from the NCDC U.S. Surface Summary of the Day historical archive. Data from NCDC undergo internal quality control prior to archiving as provided above. Mexican rainfall data are screened for missing and erroneous data values by the Servicio Meteorology Nacional (SMN). The exact methods used by SMN in their quality control procedures were not known at the time of this writing, and as such error analyses over Mexico are subject to greater uncertainty than those over the United States. Mexican and United States rain gauge locations are indicated by the small numbers in Fig. 1. From Fig. 1 it is evident that extensive regions exist (e.g., northern Mexico) where gauge density is very low. Verification analyses in such regions are subsequently subject to more uncertainty than analyses in regions with higher gauge densities.

Monthly statistics in the form of regional mean bias (bias) and regional root-mean-square error (rmse) were calculated over the physiographically similar regions shown in Fig. 1. Statistical significance at the 95% level in the intersimulation differences in regional mean biases was assessed using the nonparametric Mann–Whitney test as described in von Storch and Zwiers (1999). The regions correspond roughly to those used by Schmitz and Mullen (1996) in their analysis of water

vapor transport over the NAM region. Region 0 corresponds to the entire modeled domain, region 1 to Arizona and New Mexico, region 2 to the southern Great Plains, region 3 to the Sierra Madre Occidental and western coastal plain, region 4 to the Central Plateau, region 5 to the Sierra Madre Oriental and eastern coastal plain, and region 6 to the Balsas basin complex. This allowed regional assessment of the model error in surface climate variables.

3. Results

a. Evaluation relative to upper-level soundings

Figure 2 shows the difference between monthly average profiles of modeled and observed temperature, specific humidity, and equivalent potential temperature at the seven sounding stations. The rmse and mean bias statistics for these three variables evaluated over all stations and at all levels are given in Table 2. Statistically significant differences between mean biases, at the 95% level, are denoted by the superscript text next to each simulation title. Significance in the upper air variable differences was tested using a Student's t-test adjusted for unequal variances as described in von Storch and Zwiers (1999).

There are substantial differences as well as some common features between each station shown in Fig. 2. As reported by Gochis et al. (2000), the model run using the GR scheme consistently produces atmospheric structures that are cooler and drier than observed, especially at midlevels and at northernmost stations (e.g., TUS, DRT, GYM, and MCV). This is reflected by the overall negative biases in temperature, specific humidity, and equivalent potential temperature. Close examination of Fig. 2b shows that most of these biases are associated with underestimation of midlevel atmospheric moisture. The simulation using the BMJ scheme also tends to produce a mean atmosphere for July that is cooler and drier than observed, although less pronounced than with the GR scheme. It is clear from Table 2 that using the KF scheme yields a modeled atmosphere that most resembles observations. When averaged over all measurements, the net bias when using the KF scheme is small and is significantly better than the BMJ or the GR simulations at the 95% level.

The error profiles change considerably from site to site. There is a general tendency for all schemes to underestimate lower atmospheric humidity at the northern stations (Tucson and Del Rio), and there is a corresponding underestimation of equivalent potential temperature at these stations. There also appears to be a systematic underestimation of low-level moisture at MZT, which, when coupled with a relative cool bias, results in marked underestimations of low-level equivalent potential temperature at this site. With some exceptions, use of the BMJ and the GR schemes results in lower than observed values of temperature at the four
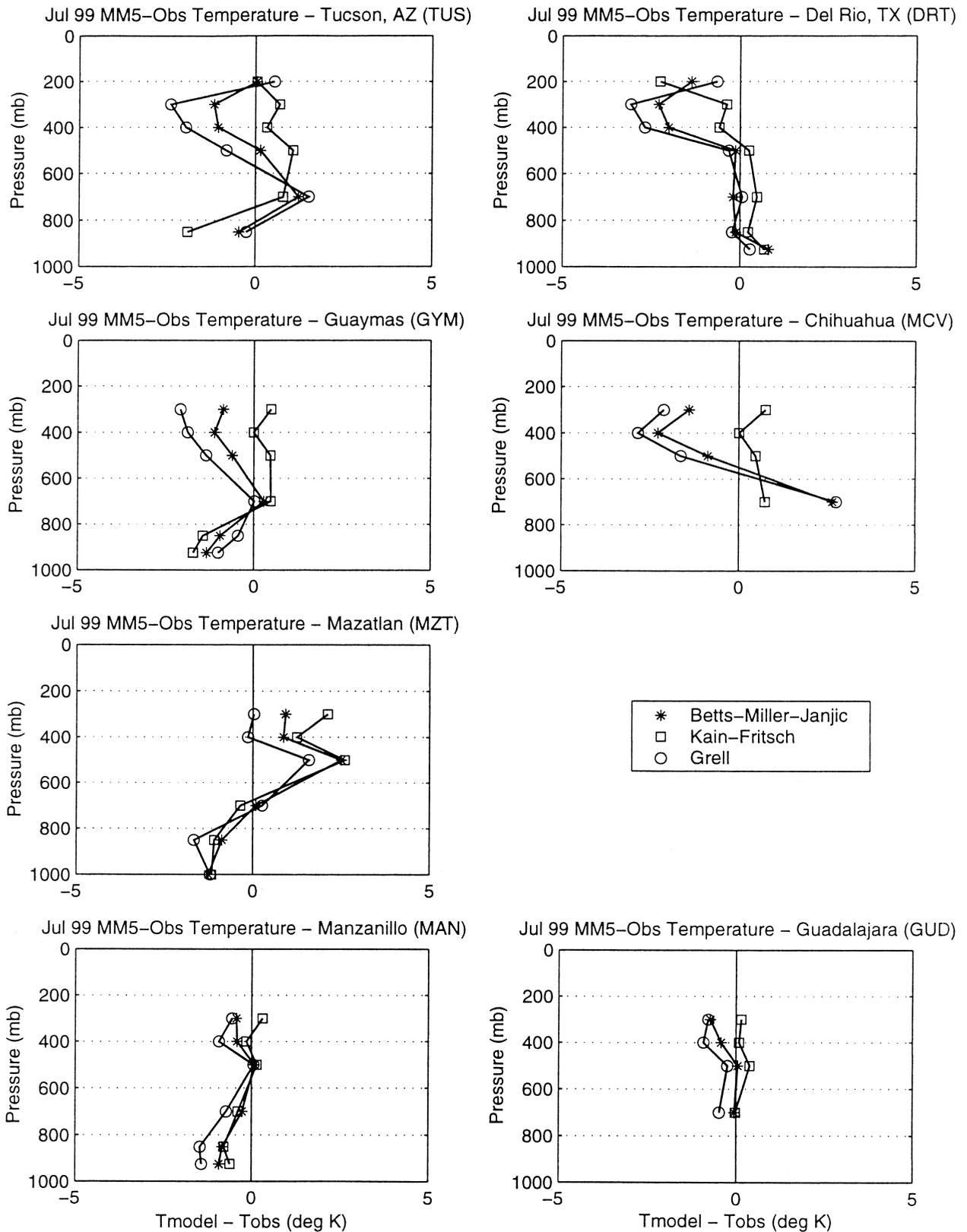
FIG. 2. Profiles of error (model–observed) of monthly mean (a) temperature (K), (b) specific humidity (kg kg^{-1}), and (c) equivalent potential temperature (K).

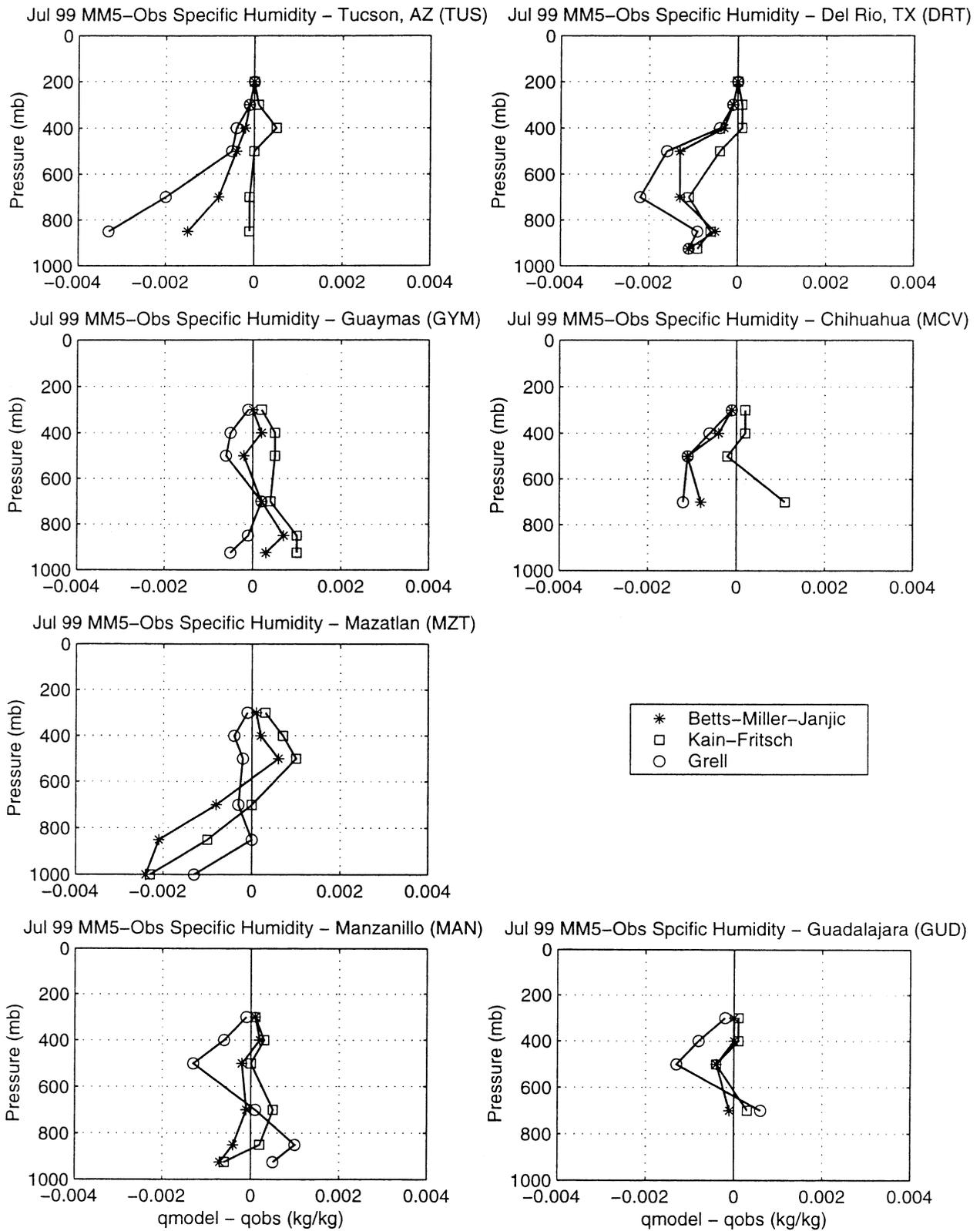FIG. 2. (*Continued*)

Jul 99 MM5–Obs Eq. Pot. Temp. – Tucson, AZ (TUS)

Jul 99 MM5–Obs Eq. Pot. Temp. – Del Rio, TX (DRT)

Jul 99 MM5–Obs Eq. Pot. Temp. – Guaymas (GYM)

Jul 99 MM5–Obs Eq. Pot. Temp. – Chihuahua (MCV)

Jul 99 MM5–Obs Eq. Pot. Temp. – Mazatlan (MZT)

* Betts–Miller–Janjic
□ Kain–Fritsch
○ Grell

Jul 99 MM5–Obs Eq. Pot. Temp. – Manzanillo (MAN)

Jul 99 MM5–Obs Eq. Pot. Temp. – Guadalajara (GUD)

Tmodel – Tobs (deg K)

Tmodel – Tobs (deg K)

Fig. 2. (Continued)

TABLE 2. Rmse and mean bias (bias) statistics for upper-level measurements. Error estimates are combined for the month of Jul from all radiosonde stations for each variable. The BMJ, KF, and GR superscripts denote simulations in which the differences in the mean bias values are significant at the 95% level.

	Temperature		Specific humidity		Theta-e	
	Rmse (K)	Bias (K)	Rmse (kg kg^{-1})	Bias (kg kg^{-1})	Rmse (K)	Bias (K)
BMJ	1.1	−0.4[KF]	0.0008	−0.004[KF]	3.1	−1.8[KF]
KF	1.0	0.1[BMJ, GR]	0.0006	0.0000[BMJ, GR]	2.6	0.3[BMJ, GR]
GR	1.4	−0.7[KF]	0.0010	−0.0006[KF]	3.8	−2.8[KF]

northernmost stations (TUS, DRT, GYM, and MCV). The midlevel atmosphere cool biases in turn yield low midlevel values of equivalent potential temperature at these sites.

Convective stability can be assessed relative to observations by examining the change in the error in equivalent potential temperature with height. Profiles of equivalent potential temperature error that become more negative with height indicate a simulated profile that is more unstable than observed, and vice versa. In most cases (except for TUS and MZT), the simulation using GR maintains a less stable atmosphere than observed, which is largely due to cooler and drier air at midlevels. Longitude–height transects of equivalent potential temperature at three different latitudes (not shown) also reveal this structure. The results using the BMJ and KF schemes do not show such a consistent tendency. Possible reasons for excess instability in the GR simulation include underestimation of convective activity due to inappropriate formulation of the trigger function or its associated parameters giving an underestimation of the convective mass flux. A more detailed discussion of this is given in section 4.

Vertical profiles of error in the u and v components of the wind (not shown) exhibit less coherence between simulations than their thermodynamic counterparts, although general tendencies do exist. All of the simulations generally underestimate the low-level, v component of the wind, this being responsible for most of the northward moisture transport in the NAM region. The only systematic exceptions are at Manzanillo, where it appeared that the prevailing wind should be more northeasterly than simulated when using all three schemes. All of the simulations also exhibited difficulty in simulating the low-level u component of the wind at northern stations (TUS, DRT, and GYM). The overestimation of low-level westerly winds at TUS and GYM and at MZT, coupled with the underestimation of the northward v component, may account for some of the underestimation of atmospheric humidity at these stations.

Verification of the model's ability to simulate the northern Gulf of California low-level jet (LLJ; not shown) was facilitated by 0000 and 1200 UTC pilot balloon measurements made at Puerto Penasco during July 1999. These (now on going) measurements are part of the Pan American Climate Studies Sounding Network (PACS-SONET 2000). All root-mean-squared error val-

ues of the v wind were in excess of the magnitude of the mean observed wind, thus indicating a serious deficiency in model simulation capability under the present configuration. In general, the diurnal amplitude of the wind at Puerto Penasco was greatly overestimated. Although the errors in the u-component wind were smaller than that of the v component, each of the three models overestimates the frequency of westerly winds relative to observations.

Figure 3 shows the 925-mb mean vector wind at 1200 UTC, along with the monthly mean column-integrated precipitable water (PW) field for the three simulations. The fields show several clear sensitivities to the convective parameterization used. The most continuous stream of northward flow occurs over the coastal plains of western Mexico in the KF simulation. Northward flow is also present to a lesser extent in the northern half of the Gulf of California (GC) in the simulation with the BMJ scheme; however, in the simulation with the GR scheme, northward winds are limited to a small region near Guaymas Bay and northwestern Sonora. All simulations show strong winds at 1200 UTC flowing from the California desert regions from northwest to southeast. This intrusion of northwesterly winds is strongest in the simulation with the GR scheme and appears to inhibit the northward advection of moisture as revealed in the PW fields. The more continuous northward flow in the simulation with the KF scheme (and concomitant deeper penetration of high PW values into southern Arizona) suggests that, in this simulation, the regional circulation is capable of tapping deeper reservoirs of atmospheric moisture from the southern GC and the eastern tropical Pacific Ocean.

Distinct differences in the modeled PW field also occur in several other regions. Integrated moisture is generally about 5–10 mm greater in the simulation with the KF scheme than with the BMJ or the GR schemes. This result, together with the significantly lower mean biases for specific humidity at upper levels (Table 2 and Fig. 2b), indicates that the simulation with the KF scheme produces a moisture atmosphere that is closer to observations than the simulations with the other two schemes. In particular, the simulations with the BMJ and GR schemes both result in marked negative biases in PW values across the northern regions of the NAM, in Arizona and New Mexico, as well as in the dry interior regions in central Mexico and southern Texas.
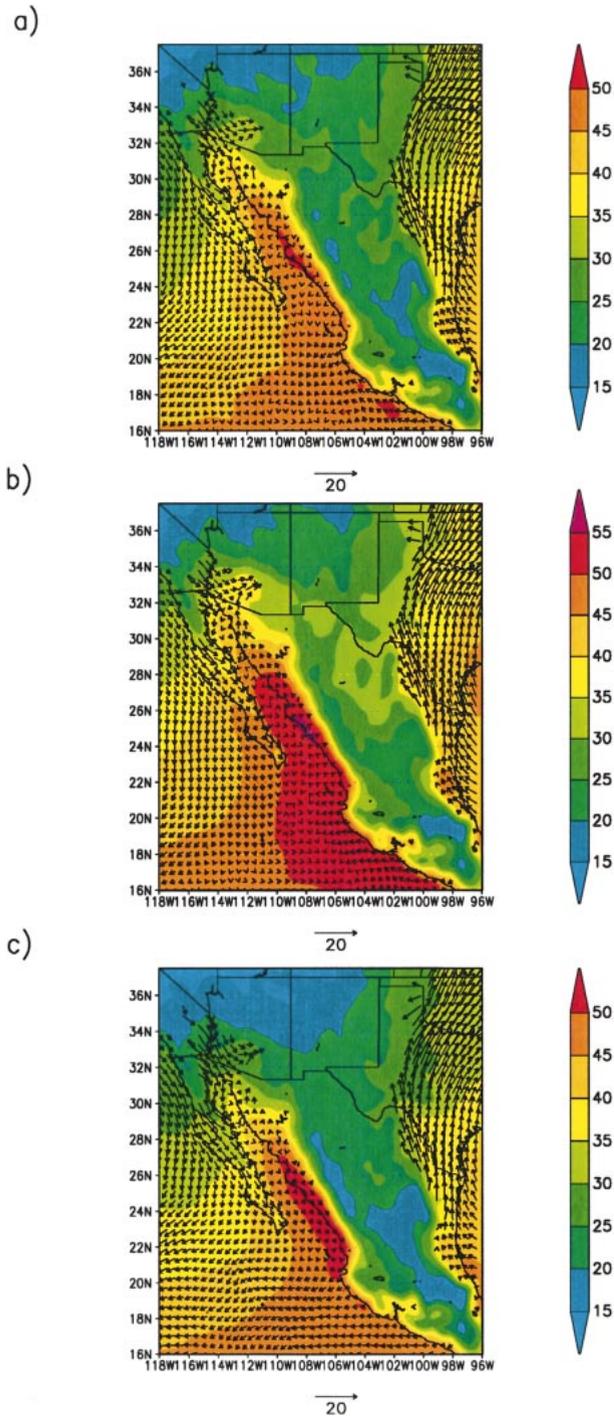
FIG. 3. The Jul mean column-integrated precipitable water content (mm) (shaded) and mean 925-mb 1200 UTC wind vectors: (a) BMJ, (b) KF, and (c) GR.

FIG. 4. The Jul mean surface–600-mb pressure-integrated divergence (s^{-1}) and mean surface–600-mb pressure-integrated streamline pattern: (a) BMJ, (b) KF, and (c) GR.

Higher PW values are also modeled in the simulation with the KF scheme across much of the southern Pacific Ocean, although these were not verified against observations such as satellite-derived PW estimates.
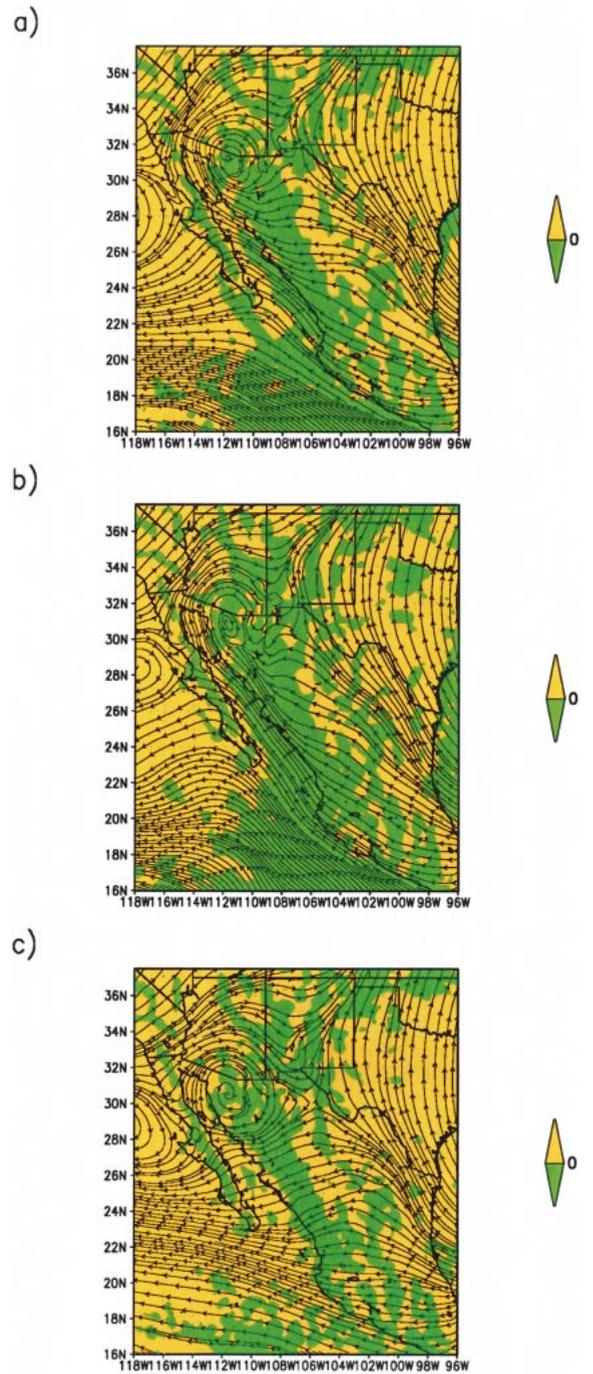
Figure 4 compares the modeled July mean surface–

600-mb pressure-integrated streamline and divergence fields for all model output times. These fields are important because they describe aspects of regional atmospheric circulation associated with the generation and sustenance of convection. Similar general patterns of convergence occur over the North American cordillera

in all three simulations, with weak divergence over the southern Great Plains, southern California, and the eastern Pacific. However, there are also distinct differences. In the KF simulation, there appears to be more extensive and weaker low-level convergence (negative divergence) over much of western Mexico that, with the BMJ and GR schemes, is largely confined to the Sierra Madre Occidental (SMO) and to high terrain in Arizona and New Mexico. Perhaps the most significant feature, however, is the streamline pattern across the GC and western Mexico. It is evident that the integrated low-level wind field in the KF simulation is able to transport moisture from well south of the mouth of the GC northward into the convective regions over the SMO and onward into southern Arizona. The BMJ simulation develops a similar flow but with a much larger westerly component than does KF. The simulation with the GR scheme develops a very different streamline pattern, which would significantly inhibit northward flow up the GC. Monthly mean profiles of the v-component wind at GYM, MZT, MAN, and GUD (discussed below and shown in Fig. 5) each reveal that the magnitude of the v wind is less in GR than in either the BMJ or KF simulation. Each simulation does, however, appear capable of producing northerly components over the far northern portion of the GC.

Although there is insufficient low-level data to verify these modeled circulation patterns, it is relevant that the limited field observations taken during the 1990 Southwest Area Monsoon Project (Reyes et al. 1994) suggest a mean, low-level wind structure similar to that found in the simulation with the KF scheme and, to a lesser degree, with the BMJ scheme. In fact, there is a notable resemblance between the KF simulation presented here and observations presented in Douglas (1995, Fig. 4a), although the northerly winds over the northern GC are farther east in the simulations with the KF and BMJ schemes. Stensrud et al. (1995) also observed a similar shift in modeled wind when using an earlier version of the MM5 model running in a 12-h assimilation–24-h forecast mode, and a similar low-level wind structure was found in regional simulations with the NCEP regional spectral model (Anderson et al. 2000). Definitive verification and explanation of the low-level wind structure in this region awaits observations proposed in the North American Monsoon Experiment (NAME) science plan (NAME 2001).

There is a perplexingly large difference between the 1200 UTC 925-mb winds shown in Fig. 3 and the surface–600-mb streamline fields given in Fig. 4. To address the question as to why this occurs we have plotted the July mean 1200 UTC, v-component winds at mandatory levels from the sounding locations of Guaymas, Mazatlan, Guadalajara, and Manzanillo against observations (see Fig. 5). It is evident that, at all sites below 600 mb, the v-component wind in the GR simulation is less in magnitude than either of the other two simulations, although not universally less than observations

(e.g., at Manzanillo). At some locations, such as Guaymas and Mazatlan, the GR-estimated v wind is of an opposite sign than either the BMJ or the KF estimates. Further, the streamline fields consist of surface–600-mb pressure-integrated wind values. This means that low-level winds are weighted more heavily than are upper-level winds within this layer. Thus, in regions where the low-level v winds in GR are underestimated or of opposite sign with respect to the other simulations, one would expect this feature to persist in integrated streamline fields. This is exceptionally evident when the profile 925-mb v winds from Mazatlan are compared.

From the v-wind profile, it is also noticed that, at both Mazatlan and Manzanillo, the magnitude of the v wind reaches a maximum at around 700 mb. In the cases of the BM and KF simulations, the upper-level winds in the surface–600-mb layer appear to have a significant influence on the integrated values due to the fact that the low-level winds are comparatively weak, being almost neutral. However, as the GR simulation fails to produce as intense magnitude v winds at upper levels anywhere in the surface–600-mb layer, its streamlines do not possess as strong a northward component. Assuming that the mean winds at the sounding locations are at least somewhat indicative of the regional winds over the eastern Gulf of California, it is suspected that these differences are the reason for the large intersimulation differences between the 925-mb level and the surface–600-mb integrated wind fields.

b. Evaluation relative to surface temperatures

Table 3 gives the regionally averaged, monthly rmse, and mean bias for the daily average temperature and dewpoint temperature at 2 m above ground level. Bold text and superscripts next to mean biases indicate significantly different intersimulation biases at the 95% level, as in Table 2. There is a distinct dry bias (i.e., lower dewpoint) in all regions and all simulations. The underestimation in T_d in Table 3 corresponds with the general underestimation of lower atmospheric humidity noticed in the previous section. However, it is important to recognize that negative biases in surface dewpoint temperature can arise from elevation discrepancies between station observations and modeled values, and that smoothed model topography tends to increase the mean valley elevations of the modeled terrain where most climate stations are located (Giorgi and Shields 1999). It is also possible that the negative bias in T_d is caused by an inaccurate representation of the planetary boundary layer (PBL) as simulated by the PBL parameterization. Poor representation of the diurnal evolution of the PBL in the northern regions of the NAMS may also contribute to negative biases in precipitation there as discussed below.

The intersimulation differences are arguably more interesting, although only the difference between the KF and GR simulations in region 1 is statistically significant
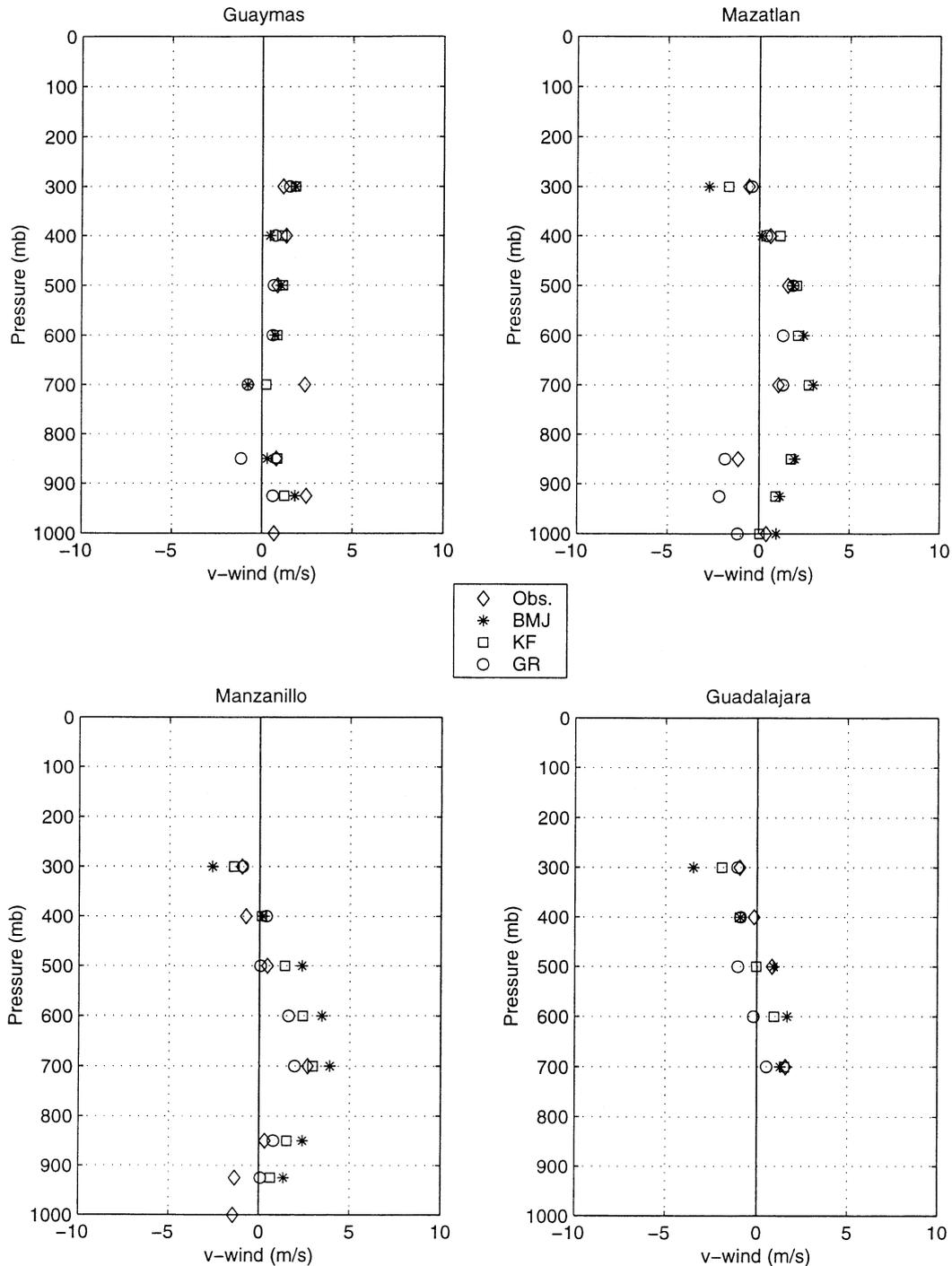
FIG. 5. Profiles of observed and model-estimated 1200 UTC monthly mean v-component winds (m s^{-1}) at mandatory levels.

at 95%. There is a substantial negative bias in T_d in the simulation with the GR scheme as reported by Gochis et al. (2000), with rather less negative bias in the simulation with the BMJ scheme. The simulation with the KF scheme consistently has the smallest rmse in T_d everywhere. Region 1, which covers Arizona and New Mexico, is the region with consistently highest errors. This underestimation in the northern portion of the NAM region reflects the modeled underestimation of northward transport of moisture into the region that was suggested by large wind errors in the pilot balloon data and the v-component wind in the soundings.

TABLE 3. Regionally averaged surface climate statistics (Rmse) and (bias) for NAM subregions. Bold text and BMJ, KF, GR superscripts denote simulations in which the differences in the mean bias values are significant at the 95% level.

Region	Bias			Rmse		
	BM	KF	GR	BM	KF	GR
Regionally averaged surface daily average dewpoint statistics (°C) Jul 1999						
0	−3.8	−2.0	−4.5	4.6	2.7	5.6
1	−6.8	−3.7[GR]	−9.2[KF]	7.0	4.4	9.5
2	−4.3	−1.9	−4.5	4.4	2.0	4.7
3	−2.5	−1.7	−2.3	2.8	1.9	2.3
4	−2.5	−0.9	−2.7	3.3	1.8	3.5
5	1.8	−1.3	−2.4	2.6	1.7	2.9
6	−1.1	−0.7	−1.4	1.4	1.1	1.6
Regionally averaged surface daily average temperature statistics (°C) Jul 1999						
0	2.0	0.7	1.8	3.0	2.1	2.8
1	1.9	−0.2	2.0	2.4	1.7	2.6
2	4.1	2.2	3.6	4.2	2.4	3.7
3	−0.4	−1.4	−0.6	0.6	1.6	0.6
4	0.5	−0.8	0.3	1.8	1.6	1.5
5	1.2	0.3	0.6	1.7	1.3	1.2
6	−0.4	−0.9	−0.3	1.3	1.4	1.3
Regionally averaged total precipitation statistics (mm) Jul 1999						
0	**17.5**[KF, GR]	**27.6**[BM, GR]	**−49.8**[BM, KF]	112.0	72.7	76.2
1	**−44.2**[KF, GR]	**6.8**[BM, GR]	**−74.6**[BM, KF]	65.1	30.5	80.5
2	**−34.5**[KF, GR]	**21.1**[BM, GR]	**−32.9**[BM, KF]	38.3	24.5	37.4
3	**171.3**[KF, GR]	**96.3**[BM, GR]	**−3.5**[BM, KF]	225.5	139.3	71.8
4	**21.6**[KF, GR]	**48.8**[BM, GR]	**−64.5**[BM, KF]	80.9	59.3	70.6
5	**−38.8**[KF, GR]	**−5.0**[BM, GR]	**−89.5**[BM, KF]	65.2	67.6	111.0
6	**169.8**[KF, GR]	**52.5**[BM, GR]	**−15.1**[BM, KF]	200.5	97.3	63.0

The error statistics for T_{av} are similar to those for T_d, although none of the intersimulation differences in mean biases are statistically significant at 95%. For this variable, the rmse in region 0 is greatest in the simulation with the BMJ scheme, followed by that with the GR, then the KF schemes. In all of the simulations, the errors are greatest in region 2 (the southern Great Plains) followed by those in region 1. There is less consistency in the rmse values for T_{av} in regions 3, 4, 5, and 6, in Mexico, than in the regions within the United States. There is a general positive bias in the maximum daily temperature (not shown) in the simulation with the GR scheme and, to a lesser extent, in the simulations with the BMJ scheme compared to that with the KF scheme. As discussed later (section 4), this is important because it supports the hypothesis that simulations with the GR and BMJ schemes allow more instability in the model climate, possibly indicating a deficiency in adequately representing the extent of convective activity in northern regions. On the other hand, the bias in T_{max} for the simulation with the KF scheme is small in all regions, with only a slight positive bias in regions 1 and 2.

c. Evaluation relative to observations of precipitation

Figure 6 shows the spatial distribution of modeled precipitation from the three simulations along with a satellite-derived estimate of precipitation from the Precipitation Estimation from Remotely Sensed Information using Artificial Neural Networks (PERSIANN) sys-

tem (Sorooshian et al. 2000). PERSIANN-estimated rainfall has been verified against the stage IV merged radar–rain gauge product over two locations in Florida and in Texas, and has been shown to yield good results although some deficiencies exist as discussed by Sorooshian et al. (2000). At the time of this writing, the accuracy of the PERSIANN estimates over the NAM region has yet to be verified, although preliminary analyses have shown that it captures well the diurnal cycle of deep convective activity over Mexcio and the southwestern United States. Clearly, the simulation with the KF scheme produces more extensive precipitation than with either the BMJ or GR schemes. There is a substantial difference in the magnitude and extent of the modeled rainfall over Arizona, New Mexico, Texas, Oklahoma, and central Mexico. The bias and rmse for precipitation given in Table 3 show that errors are lowest with the KF scheme in regions 1, 2, and 4, although this scheme slightly overestimates precipitation in these regions. Note that all intersimulation differences in regional mean biases are significant at the 95% level, as denoted by the superscripts.

Several features of the precipitation fields are worth noting. First, there appears to be substantial discrepancy in the estimation of precipitation in region 3, the core of the monsoon region along the western slopes of the SMO. The rmse statistics indicate a substantial error, with a significant positive bias in the simulation with the BMJ scheme and, to a lesser degree, the KF scheme. With the GR scheme, the rmse is less than that with
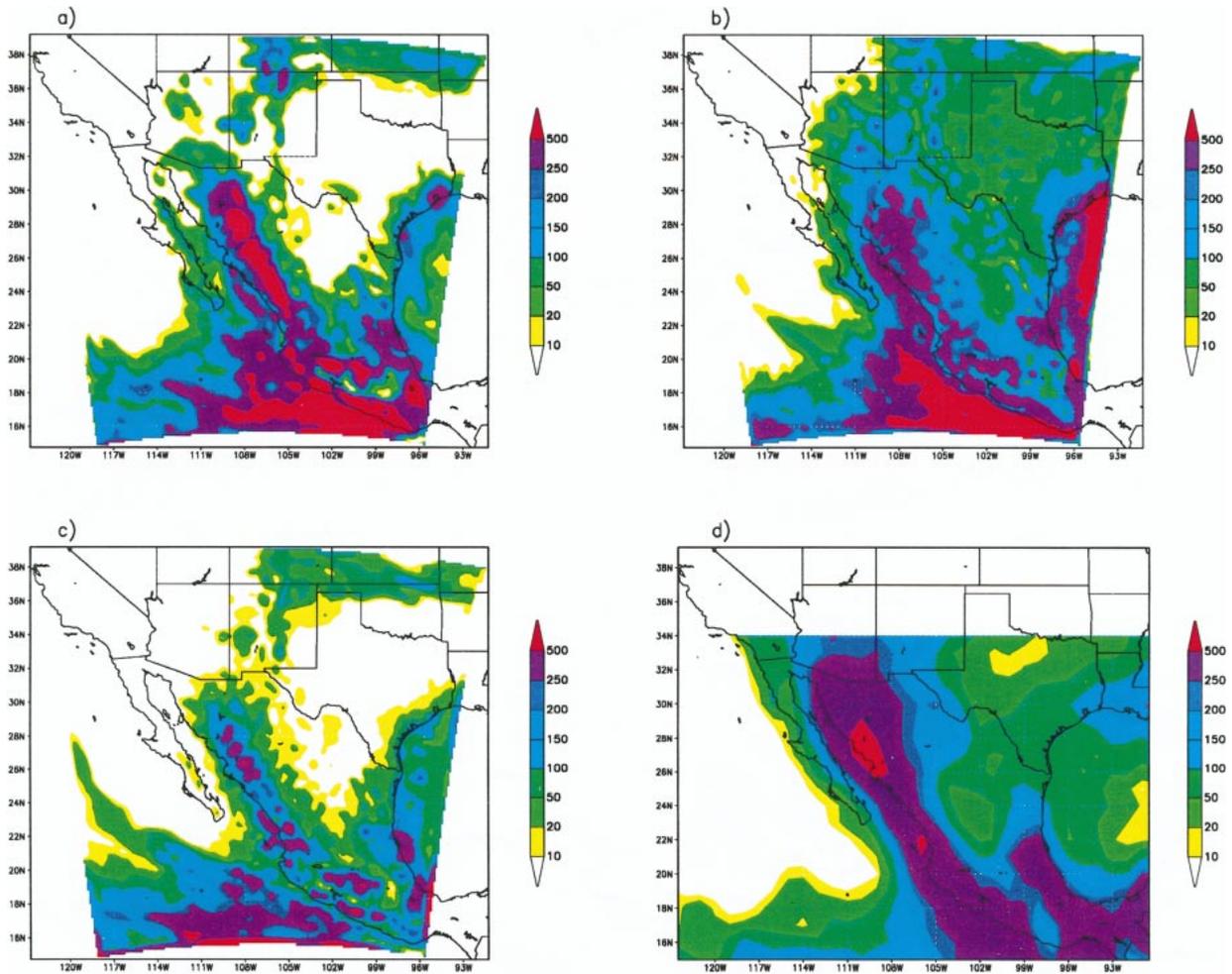
FIG. 6. The Jul total precipitation (mm) (shaded): (a) BMJ, (b) KF, (c) GR, and (d) PERSIANN.

both the BMJ and KF schemes, and its mean bias is close to zero. In the absence of reliable, high-resolution precipitation gauge data that adequately sample topography, and based on these findings, we suspect that the actual precipitation in this region is closest to that of the GR scheme. Second, KF precipitation estimates from inland regions of Mexico and the southern Great Plains verify well against the PERSIANN data.

Third, the simulation with the KF scheme appears to suffer from a boundary condition problem along the eastern boundary of the inner domain, where a monthly total precipitation in excess of 500 mm is simulated. Such a feature is not present in the PERSIANN data, and we believe that the generation of heavy precipitation here is spurious and due to interaction between the convection scheme and the model boundary condition as found in Stensrud et al. (1995). There is inflow at this boundary, and the thermodynamic structure of the imported atmosphere is largely determined by the structure on the coarse domain that uses the BMJ convection scheme. It seems likely that the excess instability present

in the BMJ scheme (suggested above) is brought into the internal domain, which is sufficient to trigger convection within the KF scheme operating in the internal domain, resulting in excessive estimates of rainfall just inside the domain boundary.

Last, there is a substantial difference in the amount of precipitation produced along the southern boundary of the internal domain and in southern Mexico in the simulations with the BMJ and KF schemes compared to GR scheme. Both the KF and the BMJ simulations appear to markedly overestimate rainfall along the southwest coast of Mexico relative to PERSIANN. This overestimation is also reflected in a substantial bias and rmse in region 6 with the BMJ and, to a lesser extent, the KF scheme. The exact cause of this feature is unknown at this writing as all three simulations produce broadly similar precipitation patterns over the ITCZ on the 90-km domain. In the case of the simulation with the KF scheme, a boundary-related process similar to that described in the previous paragraph might be the cause, but this does not readily explain the (greater)

overestimation of precipitation given with the BMJ scheme. This aspect of these simulations is the subject of ongoing study.

4. Discussion

The following points summarize the results of the analyses described above.

- Substantial differences in both the thermodynamic and circulation structure of the simulated July 1999 NAM atmosphere evolve when different CPS schemes are used.
- In addition to entire-domain error tendencies, subregional error tendencies are also prevalent, and many of the intersimulation differences are statistically significant.
- As reported by Gochis et al. (2000), the MM5 simulation using the GR scheme yields an atmosphere in July 1999 that is drier than observed in terms of lower- and upper-tropospheric moisture content and precipitation.
- MM5 simulations with both the BMJ and GR schemes give a marked underestimation of convective precipitation in the northern NAM regions, that is, in the southwestern United States, the southern Great Plains, and over the central Mexican plateau. Conversely, simulations with the KF scheme show only a slight positive bias across these same regions. Over the SMO, however, and over far southern Mexico, the GR scheme appears to best simulate the observed precipitation field.
- The error in the modeled surface dewpoint temperature field is greater in the northern monsoon regions than in other regions, regardless of the convective scheme used. The error is greatest in these regions for the simulation with the GR scheme, followed by that with the BMJ scheme, while the error with the KF scheme is least.
- Based on profiles of equivalent potential temperature, use of the GR scheme results in more instability in the atmosphere than use of the BMJ scheme, and significantly more instability than use of the KF scheme. Similarly, use of the GR scheme results in marked underestimation of the moisture and temperature at midlevels in the atmosphere compared to use of the other two schemes.
- As a result of the difference in the CPSs, markedly different regional circulation patterns evolve, which are revealed in the integrated low-level streamline and divergence fields. The KF scheme results in a broader distribution of low-level convergence, which extends into central Mexico and into the southwestern United States. In contrast, convergence is more localized and locked primarily to the highest topographic features when both the BMJ and GR schemes are used.
- Large differences occur in the mean low-level wind structure between the three simulations. The simula-

tion with the KF scheme maintains a continuous flow of southeasterly low-level wind across the GC that appears to transport moisture from far south of the mouth of the GC. While similar to KF, the flow in the BMJ simulation appears to have less of a northward component. Northward flow in the GR simulation is restricted only to the northern GC.
- Differences in the circulation fields result in markedly different fields of column-integrated precipitable water. Appreciable whole-column water vapor is advected northward into Arizona and the central Mexican plateau only when the KF scheme is used in MM5.

On the basis of the results of this study, it is evident that the representation of convection in regional climate models has a marked influence not only on model-estimated precipitation, but also on the simulated circulation patterns in the NAMS. These results support the earlier findings of Stensrud (1996), who concluded that the effects modeled persistent, deep convection over the central plains of the United States could serve to alter the low-level circulation, generate Rossby waves, and produce upper-level perturbations that extend as far as $50°$ longitude from the convective region. Although a detailed discussion on the uncertainty in convective parameterization is beyond the scope of this basic sensitivity study, a brief discussion of our simulation results is provided next.

The convective trigger function is the portion of a CPS that governs when the CPS is activated. Because the GR scheme maintains a comparatively unstable atmosphere, it seems plausible to suggest that the GR CPS is not triggered as frequently as the KF CPS during simulation. The ironic feature that the GR scheme maintains more instability while producing less rainfall is supported by large differences in the July mean fields of the high-cloud fraction (not shown), which reveal that the GR simulation produces a much smaller area of high cloud than the other two simulations. Initiation of convection in a particular region can be improved by tuning CPS parameters such as lifted depth criteria. In fact, Giorgi and Mearns (1999) recommended such tuning. However, the results may be beneficial in some regions but deleterious in others. For example, lowering the lifted-depth requirement to generate more convection in, say, Arizona may result in too much convection in southern Mexico. Perhaps this is occurring with the KF scheme, as it is overestimating precipitation in southern Mexico. It should also be noted, as discussed in Janjic (1994), that convective scheme triggering is sensitive to PBL formulation, such that different PBL formulations may either beneficially or detrimentally affect the simulation of convection.

The trigger function in the BMJ scheme also appears to inhibit convective activity in the northern NAM regions, which gives reduced precipitation and a relatively cooler and drier midlevel atmosphere compared with

the KF simulation. This is not surprising because the convective trigger formulation used in the BMJ scheme is very similar to that used in the GR scheme, that is, a lifted-depth criterion must be overcome by the large-scale vertical velocity. Where the BMJ scheme is activated, for example in regions 3 and 6, there appears to be an overestimation of precipitation. This suggests that the profile adjustment procedure used in the BMJ scheme is either yielding too much column water during the relaxation of large-scale profile toward the reference profile, or that too much of the residual moisture is being converted into precipitation. It may be acceptable to tune either the reference profile parameters or the parameters in the precipitation generation equation without degrading the overall performance of the scheme. In fact, this task is simplified by the fact that the changes made by Janjic (1994) reformulated both the reference profiles and the precipitation generation equation in terms of a "cloud efficiency" parameter. While the cloud efficiency parameter is not single valued and can evolve, depending on the large-scale environment, it may be possible to tune the formulation of cloud efficiency to produce atmospheric structures and precipitation fields more similar to observations than at present.

The KF CPS is the most physically complex representation of the three schemes considered in this study (see section 2 and the appendix). Although increased complexity does not necessarily translate into increased performance, there are attributes of the KF scheme that make it appealing when simulating convection in the NAM region. As noticed above, the KF scheme does appear to generate convective precipitation more realistically in the northern part of the NAMS than either the GR or the BMJ schemes. Moreover, the treatment of hydrometeors in the KF CPS (especially ice) ensures that exchanges of latent heat of fusion are accounted for. Ice processes are effectively neglected in the GR scheme, which may account for at least part of the observed cool bias at midtropospheric levels. No such systematic cool bias exists in the KF simulation.

Probably most important, the KF CPS includes entraining/detraining air to and from convective clouds. Although it is difficult to diagnose the effect of the cloud model formulation in the analyses presented here, such processes are likely to become more significant in the drier convective environments of southwestern Arizona and the central plateau of Mexico. The hypothetically beneficial aspects of the KF scheme are supported by the fact that, when it is used, midlevel heat and moisture profiles have statistically significant less error than do the profiles generated when the nonentraining GR scheme is used. Detrainment of convective updrafts and downdrafts is expected to be comparatively less important in southern Sinaloa than in southwestern Arizona because the moisture profiles are deeper there. The fact that the GR scheme yields lower error estimates in southern Mexico (in region 6) may suggest that representing cloud entrainment/detrainment may not necessarily be beneficial in tropical regions.

5. Conclusions

This study shows that MM5 simulates substantially different regional climates during the North American monsoon when different convective schemes are used. Although there are some common features, the comparative performance of the different schemes differs across the modeled domain. This is perhaps not surprising because different CPSs have assumptions and parameter specifications that make them more appropriate in some regions than others, but it complicates the task of using regional climate models over domains of appreciable size. Running a mesoscale model over the whole NAM region presents convective parameterization challenges beyond those faced at the meso-β scale.

The simulations described above do not represent a thorough testing of the CPSs considered in this study. Nonetheless, the conclusion that there is substantial sensitivity in model-generated climate, especially with regard to the low-level circulation, to the selection of a CPS is believed to be a robust conclusion. Such sensitivity presents an interesting challenge for long-term hydrologic prediction systems. Changes in convective parameterization can result in marked differences in the regional moisture transports into and out of a particular subregion. These circulation changes interact with changes in the local efficiency with which precipitation is released, and important feedbacks emerge that can potentially alter the modeled hydrological characteristics of a given subregion.

APPENDIX

Convective Parameterization Scheme Descriptions

a. Betts–Miller–Janjic scheme

Betts (1986) and Betts and Miller (1986) proposed a convective parameterization for deep and shallow convection based on the principle of "saturation point" thermodynamics outlined in Betts (1982). In this

scheme, profiles of temperature and moisture in a column with sufficient resolved-scale vertical motion and instability are instantaneously relaxed toward observed, quasi-equilibrium structures. The method is similar to that of Kuo (1974), except that the convective column in the Kuo scheme is relaxed toward a reference that is the moist-adiabatic profile. The difference is proposed because observational evidence suggests that using the moist-adiabatic profile yields convective available potential energy (CAPE) in excess of observed kinetic energies. The BMJ CPS does not account for subgrid cloud and mesoscale processes such as microphysical processes or updrafts and downdrafts, although release of latent heat of fusion due to ice processes is implicit in the construction of the reference profiles. Precipitation from the deep convection scheme is calculated as the residual integrated water between the large-scale moisture profile and the reference profile. Janjic (1994) substantially modified the original Betts–Miller scheme by allowing the reference profiles to vary with the convective environment, as diagnosed by a ''cloud efficiency'' parameter. These modifications are included in the current version of the Betts–Miller scheme used in the MM5 modeling system.

b. Kain–Fritsch scheme

The Kain–Fritsch convective parameterization scheme is a combination of the one-dimensional entraining/detraining plume model of Kain and Fritsch (1990) and the convective parameterization framework of Fritsch and Chappell (1980). The Fritsch and Chappell formulation is a mass flux scheme that governs the initiation of convection and convective relaxation (by which instability is removed from the grid-scale convective column), while the Kain and Fritsch portion of the scheme is a cloud model, which governs the redistribution of heat and moisture; in both liquid and solid phases. The effects of moist updrafts and downdrafts and the detrainment and subsequent evaporation/sublimation of cloud condensate into the downdraft are all explicitly represented in the KF CPS. Convection is initiated when there is a net column instability and sufficient grid-resolved, upward vertical velocity to overcome any negative buoyancy in the lower-atmospheric layers. The CAPE present on the resolved scale governs the quantity of the convective mass flux required to consume the grid-resolved CAPE over a (assumed) convective time step of approximately 1 h. Precipitation is formed within the cloud model as the mechanism by which excess cloud condensate is removed and occurs at a rate that is an inverse function of the mean layer vertical velocity and a direct function of a prescribed rate constant.

c. Grell scheme

The Grell scheme is a one-dimensional mass flux scheme that consists of a single updraft–downdraft cou-

plet. It is a highly simplified version of the Arakawa and Schubert (1974) cloud ensemble parameterization implemented as a single cloud member. Unlike in the KF CPS, there is no direct mixing between the updraft and downdraft and with the surrounding atmosphere, except at the top and bottom of the cloud. Thus, the convective mass fluxes are constant with height. Because all condensed water vapor in the convective cloud is removed as potential rainwater, there is no explicit accounting of ice processes in the GR CPS. As with the KF scheme, the convective mass flux is determined by the flux required to stabilize an unstable air column, but the closure assumptions differ in implementation between the two schemes. The Grell scheme is activated using a trigger mechanism similar to that used in the KF scheme in that it is not activated until a lifting-depth criterion is met that indicates there is sufficient lift to access potential buoyant energy. Convective precipitation is calculated as a function of the convective mass flux, the amount of cloud condensate that has been removed as rainwater but not evaporated into the downdraft, and a precipitation efficiency parameter.

REFERENCES

Adams, D. K., and A. C. Comrie, 1997: The North American monsoon. Bull. Amer. Meteor. Soc., **78,** 2197–2213.

Anderson, B. T., J. O. Roads, S.-C. Chen, and H.-M. Juang, 2000: Regional simulation of the low-level monsoon winds over the Gulf of California and southwestern United States. J. Geophys. Res., **105** (D14), 17 955–17 969.

Arakawa, A., and W. H. Schubert, 1974: Interaction of a cumulus cloud ensemble with the large-scale environment, Part 1. J. Atmos. Sci., **31,** 674–701.

Barlow, M., S. Nigam, and E. H. Berbery, 1998: Evolution of the North American monsoon system. J. Climate, **11,** 2238–2257.

Betts, A. K., 1982: Saturation point analysis of moist convective overturning. J. Atmos. Sci., **39,** 1484–1505.

——, 1986: A new convective adjustment scheme. Part I: Observational and theoretical basis. Quart. J. Roy. Meteor. Soc., **112,** 677–691.

——, and M. J. Miller, 1986: A new convective adjustment scheme. Part II: Single column tests using GATE wave, BOMEX, ATEX and arctic air-mass data sets. Quart. J. Roy. Meteor. Soc., **112,** 693–709.

Chen, F., and J. Dudhia, 2001: Coupling an advanced land surface-hydrology model with the Penn State-NCAR MM5 modeling system. Part 1: Model implementation and sensitivity. Mon. Wea. Rev., **129,** 569–585.

Copeland, J. H., R. A. Pielke, and T. G. F. Kittel, 1996: Potential climatic impacts of vegetation change: A regional modeling study. J. Geophys. Res., **101,** 7409–7418.

Dickinson, R. E., R. M. Errico, F. Giorgi, and G. T. Bates, 1989: A regional climate model for the western United States. Climatic Change, **15,** 383–422.

Douglas, M. W., 1995: The summertime low-level jet over the Gulf of California. Mon. Wea. Rev., **123,** 2334–2347.

——, R. A. Maddox, K. W. Howard, and S. Reyes, 1993: The Mexican monsoon. J. Climate, **6,** 1665–1677.

Fritsch, J. M., and C. F. Chappell, 1980: Numerical prediction of convectively driven mesoscale pressure systems. Part I: Convective parameterization. J. Atmos. Sci., **37,** 1722–1732.

Giorgi, F., 1990: On the simulation of regional climate using a limited area model nested in a general circulation model. J. Climate, **3,** 941–963.

——, and M. R. Marinucci, 1996: An investigation of the sensitivity of simulated precipitation to model resolution and its implications for climate studies. *Mon. Wea. Rev.,* **124,** 148–166.

——, and L. O. Mearns, 1999: Introduction to special section: Regional climate modeling revisited. *J. Geophys. Res.,* **104** (D6), 6335–6352.

——, and C. Shields, 1999: Tests of precipitation parameterizations available in latest version of NCAR regional climate model (RegCM) over continental United States. *J. Geophys. Res.,* **104** (D6), 6353–6357.

Gochis, D. J., Z.-L. Yang, W. J. Shuttleworth, and R. A. Maddox, 2000: Quantification of error in a pseudo-regional climate simulation of the North American Monsoon. *Proc. Second Southwest Weather Symp.,* Tucson, AZ, National Weather Service.

Grell, G. A., 1993: Prognostic evaluation of assumptions used by cumulus parameterizations. *Mon. Wea. Rev.,* **121,** 764–787.

——, J. Dudhia, and D. R. Stauffer, 1994: A description of the fifth generation Penn State/NCAR Mesoscale Model (MM5). NCAR Tech. Note NCAR/TN-380+STR, 138 pp.

Higgins, R. W., Y. Yao, and X.-L. Wang, 1997: Influence of the North American monsoon system on the U.S. summer precipitation regime. *J. Climate,* **10,** 2600–2622.

Hong, S.-Y., and H.-L. Pan 1996: Nonlocal boundary layer vertical diffusion in a medium-range forecast model. *Mon. Wea. Rev.,* **124,** 2322–2339.

Janjic, Z. I., 1994: The step-mountain eta coordinate model: Further developments of the convection, viscous sublayer, and turbulence closure schemes. *Mon. Wea. Rev.,* **122,** 927–945.

Kain, J. S., and M. Fritsch, 1990: A one-dimensional entraining/detraining plume model and its application in convective parameterization. *J. Atmos. Sci.,* **47,** 2784–2802.

Kalnay, E., and Coauthors, 1996: The NCEP/NCAR 40-Year Reanalysis Project. *Bull. Amer. Meteor. Soc.,* **77,** 437–471.

Kuo, H. L., 1974: Further studies of the parameterization of the influence of cumulus convection on large-scale flow. *J. Atmos. Sci.,* **31,** 1232–1240.

Molinari, J., and M. Dudek, 1992: Parameterization of convective precipitation in mesoscale numerical models: A critical review. *Mon. Wea. Rev.,* **120,** 326–344.

NAME, cited 2001: North American Monsoon Experiment science plan. [Available online at http://yao.wwb.noaa.gov/monsoon/NAME.html.]

PACS-SONET, cited 2000: Pan-American Climate Studies Sounding Network. [Available online at http://www.nssl.noaa.gov/projects/pacs/.]

Reyes, S., M. W. Douglas, and R. A. Maddox, 1994: El monzon del suroeste de Norteamerica (TRAVASON/SWAMP). *Atmosfera,* **7,** 117–137.

Reynolds, R. W., and T. M. Smith, 1994: Improved global sea surface temperature analyses. *J. Climate,* **7,** 929–948.

Schmitz, J. T., and S. L. Mullen, 1996: Water vapor transport associated with the summertime North American monsoon as depicted by ECMWF analyses. *J. Climate,* **9,** 1621–1634.

Seth, A., and F. Giorgi, 1998: The effects of domain choice on summer precipitation simulation and sensitivity in a regional climate model. *J. Climate,* **11,** 2698–2712.

Small, E. E., 2001: The influence of soil moisture anomalies on variability of the North American monsoon system. *Geophys. Res. Lett.,* **28,** 139–142.

Sorooshian, S., K. L. Hsu, X. Gao, H. V. Gupta, B. Imam, and D. Braithwaite, 2000: Evaluation of PERSIANN system satellite-based estimates of tropical rainfall. *Bull. Amer. Meteor. Soc.,* **81,** 2035–2046.

Stensrud, D. J., 1996: Effects of persistent, midlatitude mesoscale regions of convection on the large-scale environment during the warm season. *J. Atmos. Sci.,* **53,** 3503–3527.

——, R. L. Gall, S. L. Mullenn, and K. W. Howard, 1995: Model climatology of the Mexican monsoon. *J. Climate,* **8,** 1775–1794.

von Storch, H., and F. W. Zwiers, 1999: *Statistical Analysis in Climate Research.* Cambridge University Press, 484 pp.

Wang, W., and N. L. Seaman, 1997: A comparison study of convective parameterization schemes in a mesoscale model. *Mon. Wea. Rev.,* **125,** 252–278.

Zhang, G. J., and N. A. McFarlane, 1995: Sensitivity of climate simulations to the parameterization of cumulus convection in the Canadian Climate Centre general circulation model. *Atmos.-Ocean,* **33,** 407–446.